JACS
JOURNAL OF THE AMERICAN CHEMICAL SOCIETY

Article

pubs.acs.org/JACS

Pattern Recognition Correlating Materials Properties of the Elements to Their Kinetics for the Hydrogen Evolution Reaction

Kevin C. Leonard[†] and Allen J. Bard*

Center for Electrochemistry, Department of Chemistry and Biochemistry, University of Texas at Austin, Austin, Texas 78712, United States

Supporting Information

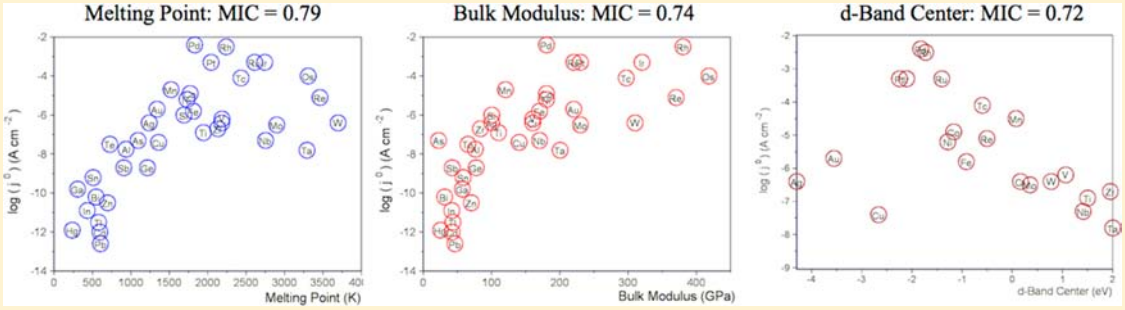

ABSTRACT: Here we demonstrate the use of a previously reported pattern recognition algorithm to evaluate correlations between 50 different materials properties of the elements and their kinetics for the hydrogen evolution reaction in acid. We determined that the melting point and bulk modulus of the elements quantitatively gave the highest correlations of all materials properties investigated. We also showed that the melting point and bulk modulus correlations held true for a popular hydrogen evolution catalysts alloy, NiMo, and a previously untested material, $MoSi_2$. In addition, we quantified the previously known relationship between the d-band center of an element and its kinetics for hydrogen evolution, and found that the melting point and bulk modulus correlations have correlations that are similar to but slightly stronger than those of the d-band center.

INTRODUCTION

Electrocatalysis is a crucial component for several energy technologies related to one of the most pertinent technical challenges—discovering new ways to capture, convert, and store renewable energy utilizing solely earth-abundant materials. Examples of electrocatalysis in energy applications include the hydrogen and oxygen evolution reactions (HER and OER) for solar fuels[1] and the oxygen reduction reaction (ORR) for fuel cells[2] and metal−air batteries.[3] To date, the best electrocatalysts for these reactions are still composed of noble metals. Although there has been considerable research into finding efficient, earth-abundant electrocatalysts for these reactions[4−8] and the study of electrocatalysis has been ongoing for over a century,[9] there are few guidelines governing which materials properties correlate to catalytic activity that can be used to screen effectively and predict new catalysts.

One guideline, demonstrated by Trasatti, Parsons, and others,[10−13] is that "volcano plots" can be drawn relating the exchange current density of the elements for the HER in acid either to a calculated metal−hydrogen (M−H) bond strength derived by Krishtalik[14] or to the free energy of the adsorption of hydrogen.[11] More recently, Nørskov, Schmickler, and others have also shown that the electrocatalytic activities of the elements for several electrochemical reactions (ORR, OER, HER, etc.), plotted vs the binding energy or free energy of adsorption of surface intermediates (determined by various density functional theory (DFT) calculations), are, in-fact, related.[15−21] These are important relationships because the HER can occur through two separate pathways (the Volmer−Tafel or the Volmer−Heyrovsky mechanism), both of which involve hydrogen atoms adsorbed on the electrode surface, H_{ads}.[11,15,22] Detailed discussions on the specifics and validity of volcano relationships appear elsewhere;[11,19,22,23] however, very generally, these volcano relations state that materials with low adsorption energies H_{ads} result in very low surface coverage of the intermediate, and thus have slow kinetics for the HER. The volcano relations also indicate that materials with high H_{ads} also result in slow kinetics because the protons are bound too tightly to the surface. Thus, the best catalysts are the ones in which the bonding energy is "intermediate"; i.e., there exists an optimum value for the free energy of adsorption where the catalytic activity is at a maximum—the peak of the volcano relationship.

In addition, as summarized by Petrii and Tsirlina,[24] others have attempted to correlate different properties to the catalytic activity of hydrogen evolution, including the electron work-function,[25] atomic number,[13] and crystal structure.[26] Both Kita[13] and Kuhn et al.[27] reported that some relationship exists between the electrocatalytic activity for the HER and the heat of atomization of the element. However, in this study, we took

Received: July 18, 2013
Published: September 24, 2013

   dx.doi.org/10.1021/ja407394q | J. Am. Chem. Soc. 2013, 135, 15885−15889

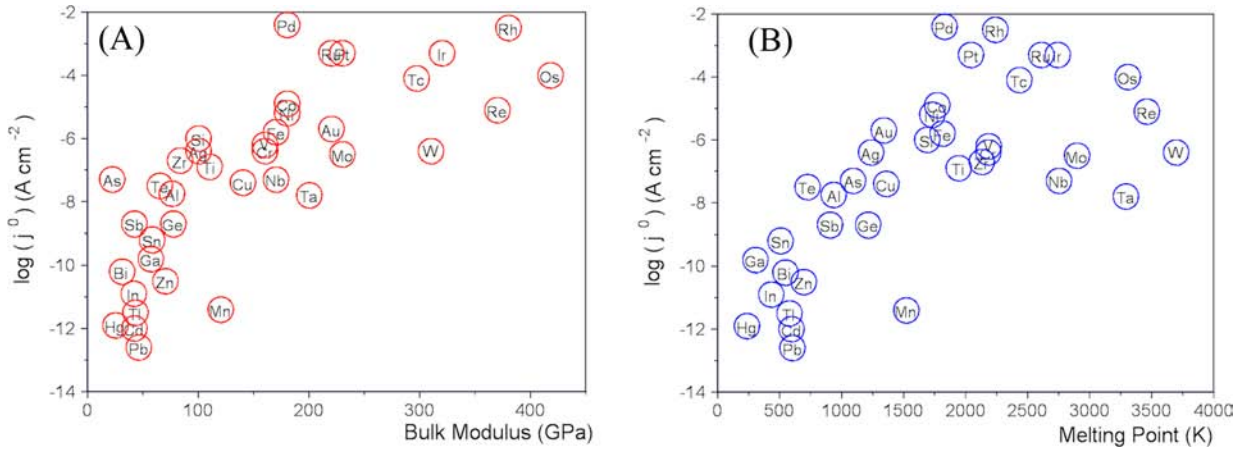

Figure 1. Log(j^0) for the hydrogen evolution reaction in acid vs (A) bulk modulus and (B) melting point for the elements. Bulk modulus showed the highest correlation of all properties tested, with a MIC value of 0.76, and melting point had the second highest correlation of all properties tested, with a MIC value of 0.71.

another approach and quantitatively investigated correlations between the bulk materials properties, mainly of the elemental metals, and their electrocatalytic activity. An improved understanding between materials properties and catalytic activity would aid in predicting and screening new earth-abundant electrocatalysts. Recently, Reshef et al.[28] developed a pattern recognition algorithm that can uncover two-variable relationships, which can be both functional and nonfunctional. The Reshef algorithm produces a maximum information coefficient (MIC), such that 0 < MIC < 1, which quantifies the goodness of correlation between the two variables.[28] MIC values will tend toward 1 for good correlations, i.e., all "never-constant noiseless functional relationships",[28] and MIC values will tend toward 0 for poor correlations or "statistically independent variables".[28]

To provide a more complete investigation on whether materials properties of the elements can be related to electrocatalytic activity, we compared the HER kinetics in acidic solution for 38 elements to 50 bulk materials properties. The HER was chosen as the test case because it has been widely studied as an inner-sphere electrochemical electron-transfer reaction with exchange current densities, j^0, that span over 10 orders of magnitude for the elements. This allows for large differences in catalytic activity to compare to the different materials properties. Moreover, there is a wealth of kinetic data available for the HER.[5] Finally, it is a pertinent reaction in the development of solar fuels, and by successfully identifying patterns relating materials properties of elements and their HER kinetics, we could develop parameters for searching for new complex HER electrocatalysts composed of earth-abundant materials.

RESULTS AND DISCUSSION

We use the base-10 logarithm of the exchange current density, log(j^0), as the figure of merit for the electrocatalytic activity for the HER in the pattern recognition analysis. All values for log(j^0) were taken from a single source[5] which summarized the HER exchange current densities of the elements in acid solution from numerous authors. The materials properties for the elements were compiled from three additional sources.[29−31] Using these four sources, a custom database was created listing the exchange current density and the 50 materials properties for 38 elements. A full list of all materials properties investigated is included in the Supporting Information (Table S1). The Reshef algorithm was applied to the custom database using all default parameters to investigate patterns between the materials properties and the exchange current density.

The Reshef algorithm found, via the resulting MIC values, that a few materials properties correlated very well to exchange current density for the HER, while other properties showed no correlation. A full list of the MIC values for all reported properties is shown in Table S1. The top two properties which most strongly correlate to log(j^0) for the HER were bulk modulus and melting point, which had MIC scores of 0.76 and 0.71, respectively. The enthalpy of atomization, mentioned above as a relationship reported by Kita[13] and Kuhn et al.,[27] ranked third, with a MIC value of 0.68. Figure 1 shows log(j^0) vs bulk modulus and melting point for the elements investigated. In general, the relationship between log(j^0) and bulk modulus (Figure 1A) shows a steep increase in log(j^0) with increasing bulk modulus in the range of 0−180 GPa. Above ∼180 GPa the relationship between bulk modulus and log(j^0) begins to plateau. The relationship between log(j^0) and melting point (Figure 1B) is volcano-type, where the elements with the highest exchange current densities lie within the melting point range of 1800−2750 K. For comparison, examples of two properties, electrical resistivity and thermal conductivity, with low MIC values, 0.30 and 0.38, respectively, are shown in the Supporting Information (Figure S1).

Examination of Figure 1 shows that Mn is an outlier for both properties, with the exchange current density for Mn being ∼7 orders of magnitude lower than what would be predicted by the two patterns. To understand this difference, one must look at the route for hydrogen evolution on Mn. Hydrogen evolution can occur by two different routes, depending on the applied potential. At less negative potentials, proton reduction occurs to produce hydrogen (reaction 1), but at more negative potentials, direct water reduction occurs (reaction 2).

$$\text{Proton Reduction:} \quad 2H^+ + 2e^- \rightarrow H_2$$
$$E^0 = 0.0 \text{ V vs. NHE} \qquad (1)$$

$$\text{Water Reduction:} \quad 2H_2O + 2e^- \rightarrow H_2 + 2OH^-$$
$$E^0 = -0.83 \text{ V vs. NHE} \qquad (2)$$

dx.doi.org/10.1021/ja407394q | J. Am. Chem. Soc. 2013, 135, 15885−15889

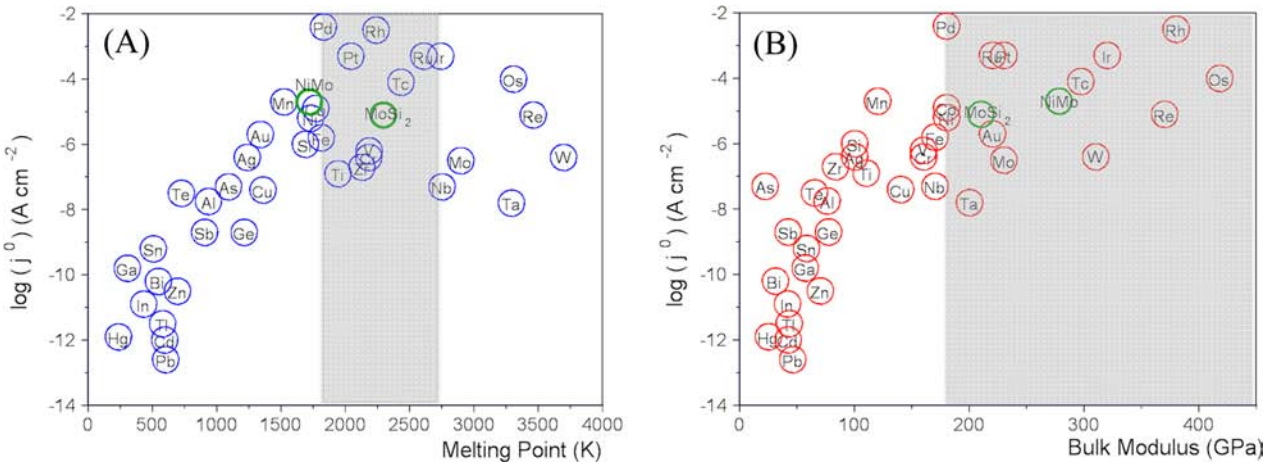

Figure 2. Log(j^0) for the hydrogen evolution reaction in acid vs (A) melting point and (B) bulk modulus for the elements using the measured value for proton reduction on Mn. Here, melting point showed the highest correlation of all properties tested, with a MIC value of 0.79, and bulk modulus had the second highest correlation of all properties tested, with a MIC value of 0.74. Bands (gray regions) are shown which outline the optimum ranges for melting point (1800−2750 K) and bulk modulus (≥180 GPa). The plots also include an HER catalyst alloy, NiMo, and a previously untested compound, $MoSi_2$, showing that both follow the melting point and bulk modulus patterns.

An example of these two reactions on a Pt ultramicroelectrode in 0.1 M NaCl + 0.01 M HCl is shown in the Supporting Information (Figure S2). Here proton reduction begins near the thermodynamic potential, and, after a diffusion-controlled limiting current is reached, an additional current increase occurs at potentials more negative than −1.2 V vs Ag/AgCl. The water reduction occurs by reaction 2 in the more local alkaline environment near the electrode.

The reported value for hydrogen evolution on Mn was for water reduction and not proton reduction.[32] This is because Mn is one of the most corrosive elements, with Mn oxidation also occurring at very negative potentials (reaction 3).

$$\text{Mn Oxidation:} \quad \text{Mn} \rightarrow \text{Mn}^{2+} + 2e^- \qquad E^0 = -1.18 \text{ V vs. NHE} \tag{3}$$

Thus, for Mn to remain stable and not undergo oxidation, the potential must be more negative than −1.18 V vs. NHE. Using conventional techniques, it is not possible to measure proton reduction on Mn in the absence of a very large corrosion current for Mn. To keep Mn from oxidizing, the potential must be held in the water reduction regime.[32]

To measure proton reduction on Mn to determine if Mn indeed does not follow the bulk modulus and melting point relationships, we developed a new multireactional tip generation/substrate collection mode of scanning electrochemical microscopy (SECM) to obtain the proton reduction kinetics on Mn in acid. The details of this technique are reported separately.[33] Using this new mode of SECM, we determined log(j^0) for the HER in acid on Mn to be −4.7 ± 0.7 A cm^{-2}.

Figure 2 shows the melting point and bulk modulus relationships using this newly measured value of log(j^0) for Mn. By using the kinetics for the proton reduction reaction instead of the water reduction reaction, the fit for Mn improves for both relationships. Also, the correlation with melting point now results in the highest MIC value of all properties tested, at 0.79, with bulk modulus having the second highest MIC value, at 0.74.

On the basis of the relationships between log(j^0) and melting point and bulk modulus, we can select optimum ranges for these two properties where the highest performing metals lie. Shown by the gray bands in Figure 2, the optimum range for melting point is 1800−2750 K, and the optimum range for bulk modulus is ≥180 GPa. Only six elements—Pd, Rh, Ir, Pt, Ru, and Tc—have melting points and bulk moduli which lie within both of the optimum ranges. Shown in the Supporting Information (Table S2) is a list of all elements investigated, ranked in order of exchange current density with the corresponding melting points and bulk moduli. The six elements that fall within both optimum ranges are ranks 1−5 and 7.

The elements that lie within the optimum band of melting points can be divided into two distinct groups on the basis of their HER kinetics. One group, consisting of Pd, Pt, and Rh, has fast kinetics for the HER, while the other group, containing Fe, Ti, V, Cr, and Zr, has slower kinetics for the HER, even though they all have similar melting points. One reason for this may be that none of the elements in the second group has a bulk modulus in the optimum range, and both materials properties appear to be important in determining good electrocatalysts for the HER. A second reason may be crystal structure. Figure 3 shows the elements with melting points above 1800 K, i.e., the peak of the volcano plot, marked by arrows designating their crystal structure.[34] In general, the elements with face-centered cubic crystal structures had the fastest kinetics for the HER, followed closely by elements with hexagonal close-packed crystal structures. Elements with body-centered cubic crystal structures tended to have slower kinetics for the HER compared to the other two crystal structures. This relationship may demonstrate the importance of atom spacing in hydrogen evolution kinetics. Since the HER data were from polycrystalline samples, crystal structures that are either face-centered cubic or hexagonal close-packed have a higher probability of having lattice planes with more closely packed atoms than body-centered cubic crystal structures.

In addition to the elements, we also investigated if these patterns would hold true for a popular HER electrocatalyst alloy, NiMo, consisting of ∼85% Ni with ∼15% Mo.[7,35−37] NiMo has a reported log(j^0) = −4.7 A cm^{-2} for proton reduction in strong acid,[37] resulting in a catalytic activity for HER just below those of the best noble metal catalysts. Figure 2

dx.doi.org/10.1021/ja407394q | J. Am. Chem. Soc. 2013, 135, 15885−15889

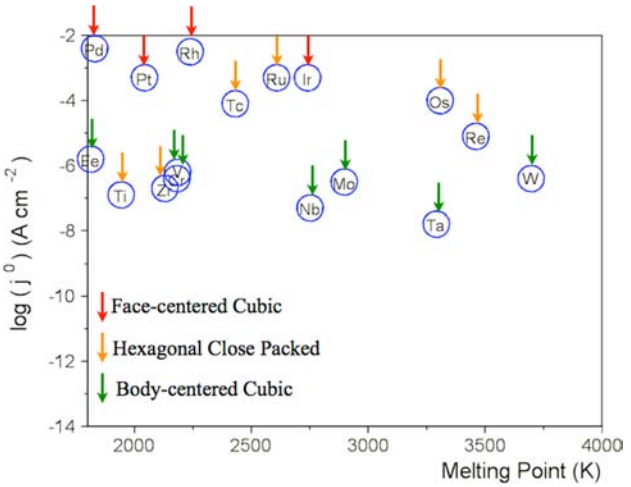

Figure 3. Log(j^0) for the hydrogen evolution reaction in acid vs melting point for the elements with melting points >1800 K. Here, the room-temperature crystal structure[24] is designated by an arrow above each point. In general, face-centered cubic crystal structures have the fastest kinetics for hydrogen evolution, followed by hexagonal close-packed structures, with body-centered cubic structures having the slowest kinetics for hydrogen evolution.

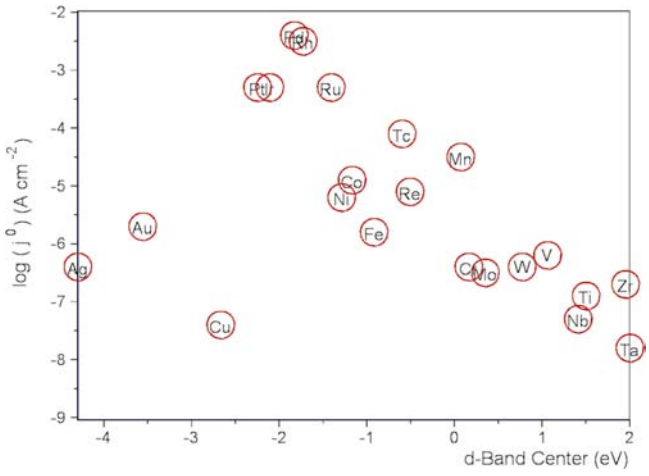

Figure 4. Log(j^0) for the hydrogen evolution reaction in acid vs d-band center for the elements.[44] Using the Reshef algorithm, log(j^0) vs d-band center has a MIC value of 0.72, ranking it third among all properties behind melting point and bulk modulus.

shows NiMo on the plots correlating log(j^0) to melting point and bulk modulus. The melting point for NiMo is 1718 K,[38] just outside the optimum range of melting point, but its bulk modulus of 278 GPa[39] and its face-centered cubic crystal structure[36] are in the optimum ranges, making for a very good fit with the rest of the elements.

We also wanted to test a compound for which the kinetics for the HER had not been previously tested, and which has a melting point and bulk modulus in the optimum range. $MoSi_2$ is a conductive compound with a melting point of 2293 K, a bulk modulus of 210 GPa, and a body-centered tetragonal crystal structure.[40] On the basis of our models, we would predict this material to have a log(j^0) higher than those of body-centered crystal structure elements such as V, W, or Mo (with log(j^0) = −6.2, −6.4, and −6.5 A cm^{-2}, respectively) because both properties are in the optimum range, but lower than for face-centered cubic elements that lie within both optimum ranges (such as Pd, Pt, or Ru with log(j^0) = −2.4, −3.3, and −3.3 A cm^{-2}). Linear sweep voltammograms for Pt, glassy carbon, and $MoSi_2$ are shown in the Supporting Information (Figure S3), with the corresponding Tafel fits. Here we found that $MoSi_2$ has a log(j^0) in acid of −5.1 A cm^{-2}, corresponding to what we would expect on the basis of its materials properties (Figure 2).

Another proposed correlation for electrocatalysts compares the energy of the d-band center of the element to electrocatalytic activity, although its validity has been challenged for correlating a wide range of metals for many electrocatalytic reactions.[41−43] To compare the pattern between d-band center and electrocatalytic activity for the HER to our materials properties trends, we show the d-band center for the most close-packed surface of the elements[44] vs exchange current density for HER in acid (Figure 4). Using the Reshef algorithm, d-band center vs log(j^0) gives a MIC value of 0.72, which would rank it third among all properties investigated, behind only melting point (MIC = 0.79) and bulk modulus (MIC = 0.74). It should be noted that, since we wanted to obtain the d-band centers from a single source, we were only able to obtain d-band centers for 22 elements, as opposed to the 38 elements whose melting points and bulk modulus data we were able to obtain. This different sample size may have some bearing on the differences in MIC values.

One can understand these correlations in terms of bonding. The properties of metals, such as melting point, strength, and atomization energy, are related to the bond strength of the metal.[34,45] In addition, the bonding energy of a metal is then related to the number of unpaired electrons available for bonding.[34] The fact that materials properties such as melting point and bulk modulus give correlations to the kinetics for hydrogen evolution, as do the energies of d-band centers, might be expected. However, these variables, e.g., melting point, are readily obtained by simple measurements, so this sort of prediction of electrocatalytic behavior by pattern recognition may be useful in the screening and discovery of new electrocatalysts.

■ CONCLUSION

We demonstrate that correlations exist between the materials properties of the elements and their kinetics for the hydrogen evolution reaction. Using the Reshef algorithm, we were able to quantify these correlations and determine that melting point and bulk modulus gave the strongest correlations of all materials properties investigated. This also allowed us to correct the literature value for the HER kinetics on Mn. We also showed that the melting point and bulk modulus correlations held true for a popular HER electrocatalyst, the alloy NiMo, and a previously untested material, $MoSi_2$. In addition, we quantified the previously known relationship between the d-band center of the element and its kinetics for the HER, and found that the melting point and bulk modulus correlations have correlations that are similar to but slightly stronger than those of the d-band center.

■ ASSOCIATED CONTENT

Supporting Information

Tables of materials properties and elements investigated, and other experimental details. This material is available free of charge via the Internet at http://pubs.acs.org.

AUTHOR INFORMATION

Corresponding Author

ajbard@mail.utexas.edu

Present Address

[†]K.C.L.: Center for Environmentally Beneficial Catalysis, Department of Chemical & Petroleum Engineering, The University of Kansas, Lawrence KS 66045

Notes

The authors declare no competing financial interest.

ACKNOWLEDGMENTS

This work was funded by the Fondazione Oronzio e Niccolò De Nora Fellowship in Applied Electrochemistry (K.C.L.), the Department of Energy (DE-FG02-09ER16119), and the Robert A. Welch Foundation (F-0021). We are indebted to Drs. W. Schmickler and T. Mallouk for very helpful suggestions.

REFERENCES

(1) Gray, H. B. *Nat. Chem.* **2009**, *1*, 7.
(2) Jaouen, F.; Proietti, E.; Lefèvre, M.; Chenitz, R.; Dodelet, J.-P.; Wu, G.; Chung, H. T.; Johnston, C. M.; Zelenay, P. *Energy Environ. Sci.* **2011**, *4*, 114−130.
(3) Capsoni, D.; Bini, M.; Ferrari, S.; Quartarone, E.; Mustarelli, P. *J. Power Sources* **2012**, *220*, 253−263.
(4) Azzam, A. M.; Bockris, J. O. M.; Conway, B. E.; Rosenberg, H. *Trans. Faraday Soc.* **1950**, *46*, 918.
(5) Appleby, A. J.; Chemla, M.; Kita, H.; Bronoel, G. Hydrogen. In *Encyclopedia of Electrochemistry of the Elements*, Vol. *IX-A*; Bard, A. J., Ed.; Marcel Dekker: New York, 1982; pp 416−456.
(6) Kanan, M. W.; Nocera, D. G. *Science* **2008**, *321*, 1072−1075.
(7) McKone, J. R.; Warren, E. L.; Bierman, M. J.; Boettcher, S. W.; Brunschwig, B. S.; Lewis, N. S.; Gray, H. B. *Energy Environ. Sci.* **2011**, *4*, 3573.
(8) Trasatti, S. Electrocatalysis of Hydrogen Evolution: Progress in Cathode Activation. In *Advances in Electrochemical Science and Engineering*, Vol. *2*; Gerischer, H., Tobias, C. H., Eds.; VCH: New York, 1992; pp 1−85.
(9) Tafel, J. *Z. Phys. Chem.* **1905**, *50*, 641.
(10) Trasatti, S. *J. Electroanal. Chem.* **1972**, *39*, 163.
(11) Parsons, R. *Trans. Faraday Soc.* **1958**, *54*, 1053−1063.
(12) Gerischer, H. *Bull. Soc. Chim. Belg.* **1958**, *67*, 506−527.
(13) Kita, H. *J. Electrochem. Soc.* **1966**, *113*, 1095−1111.
(14) Krishtalik, L. I. *Russ. J. Phys. Chem.* **1960**, *34*, 53.
(15) Rossmeisl, J.; Logadottir, A.; Nørskov, J. K. *Chem. Phys.* **2005**, *319*, 178−184.
(16) Nørskov, J. K.; Rossmeisl, J.; Logadottir, A.; Lindqvist, L.; Kitchin, J. R.; Bilgaard, T.; Jonsson, H. *J. Phys. Chem. B* **2004**, *108*, 17886−17892.
(17) Nørskov, J. K.; Bligaard, T.; Logadottir, A.; Kitchin, J. R.; Chen, J. G.; Pandelov, S.; Stimming, U. *J. Electrochem. Soc.* **2005**, *152*, J23.
(18) Greeley, J.; Jaramillo, T. F.; Bonde, J.; Chorkendorff, I. B.; Nørskov, J. K. *Nat. Mater.* **2006**, *5*, 909−913.
(19) Santos, E.; Quaino, P.; Schmickler, W. *Phys. Chem. Chem. Phys.* **2012**, *14*, 11224−11233.
(20) Koper, M. T. *Chem. Sci.* **2013**, *4*, 2710−2723.
(21) Walter, M. G.; Warren, E. L.; McKone, J. R.; Boettcher, S. W.; Mi, Q.; Santori, E. A.; Lewis, N. S. *Chem. Rev.* **2010**, *110*, 6446−6473.
(22) Schmickler, W.; Trasatti, S. *J. Electrochem. Soc.* **2006**, *153*, L31.
(23) Nørskov, J. K.; Bligaard, T.; Logadottir, A.; Kitchin, J. R.; Chen, J. G.; Pandelov, S.; Stimming, U. *J. Electrochem. Soc.* **2006**, *153*, L33.
(24) Petrii, O. A.; Tsirlina, G. A. *Electrochim. Acta* **1994**, *39*, 1739−1747.
(25) Conway, B. E.; Bockris, J. O. *J. Chem. Phys.* **1957**, *26*, 532.
(26) Vijh, A. K. *J. Electrochem. Soc.* **1971**, *118*, 263−264.
(27) Kuhn, A.; Mortimer, C.; Bond, G.; Lindley, J. *J. Electroanal. Chem. Interfacial Electrochem.* **1972**, *34*, 1−14.
(28) Reshef, D. N.; Reshef, Y. A.; Finucane, H. K.; Grossman, S. R.; McVean, G.; Turnbaugh, P. J.; Lander, E. S.; Mitzenmacher, M.; Sabeti, P. C. *Science* **2011**, *334*, 1518−1524.
(29) *Lange's Handbook of Chemistry*, 16th ed.; McGraw-Hill Professional Publishing: New York, 2005.
(30) Winter, M. WebElements: The Periodic Table on the Web. http://www.webelements.com (accessed Feb 8, 2012).
(31) Matweb Material Property Data. http://www.matweb.com (accessed March 8, 2012).
(32) Belanger, A.; Vijh, A. *J. Electrochem. Soc.* **1974**, *121*, 225−230.
(33) Leonard, K. C.; Bard, A. J. *J. Am. Chem. Soc.* **2013**, DOI: 10.1021/ja407395m, (following paper in this issue).
(34) Jolly, W. L. *Modern Inorganic Chemistry*, 2nd ed.; McGraw-Hill: New York, 1991.
(35) Warren, E. L.; Mckone, J. R.; Atwater, H. A.; Gray, H. B.; Lewis, N. S. *Energy Environ. Sci.* **2012**, *5*, 9653−9661.
(36) Huot, J. Y.; Trudeau, M. L.; Schulz, R. *Energy Environ. Sci.* **1991**, *138*, 1316−1321.
(37) Navarro-Flores, E.; Chong, Z.; Omanovic, S. *J. Mol. Catal. A: Chem.* **2005**, *226*, 179−197.
(38) Goodfellow Corp. Website. http://www.goodfellow.com (accessed Apr 2, 2013).
(39) Arya, A.; Kulkarni, U. D.; Dey, G. K.; Banerjee, S. *Metall. Mater. Trans. A* **2007**, *39*, 1623−1629.
(40) Nakamura, M.; Matsumoto, S.; Hirano, T. *J. Mater. Sci.* **1990**, *25*, 3309−3313.
(41) Hofmann, T.; Yu, T. H.; Folse, M.; Weinhardt, L.; Bär, M.; Zhang, Y.; Merinov, B. V.; Myers, D. J.; Goddard, W. A.; Hofmann, C. H. *J. Phys. Chem. C* **2012**, *116*, 24016−24026.
(42) Abild-Pedersen, F.; Nilsson, A.; Nørskov, J. K. *J. Phys. Chem. C* **2013**, *117*, 6914−6915.
(43) Hofmann, T.; Yu, T. H.; Folse, M.; Weinhardt, L.; Bär, M.; Zhang, Y.; Merinov, B. V.; Myers, D. J.; Goddard, W. A.; Hofmann, C. H. *J. Phys. Chem. C* **2013**, *117*, 6916−6917.
(44) Hammer, B.; Nørskov, J. K. *Adv. Catal.* **2000**, *45*, 71−129.
(45) Brewer, L. *Science* **1968**, *161*, 115−122.